American Mineralogist, Volume 78, pages 8–15, 1993

Local electronic states of Fe^{2+} ions in orthopyroxene

CHUANYI LIN,* LI ZHANG,** S. S. HAFNER
Institute of Mineralogy, University of Marburg, Meerwein Straße, 3550 Marburg, Germany

ABSTRACT

Resonant absorption spectra (Mössbauer effect) of ^{57}Fe in two synthetic orthopyroxenes with compositions $Fe^{2+}/(Fe^{2+} + Mg) = x = 0.80$ (Opx6) and $x = 0.51$ (Opx4) were studied at temperatures between 7 and 293 K. Opx6 showed a transition to a magnetic phase, the Néel point being $T_N = 28$ K. Opx4 did not reveal a T_N. Instead, gradually increasing magnetic line broadening occurred below $T = 12$ K because of paramagnetic relaxation.

The temperature dependencies of the nuclear quadrupole splittings, ΔE_Q, of Fe^{2+} at both M1 and M2 sites were determined. They are interpreted in terms of crystal field theory using the strong field scheme. Spin-orbit coupling and fourth-order terms were included in the calculation. For Fe^{2+} at M2, a pseudosymmetry of *mm*2 was assumed. Using the covalency factor α^2, $ze^2\langle r^2\rangle$, and $ze^2\langle r^4\rangle$ as adjustable parameters to fit the ΔE_Q data, a frequency of 817 cm^{-1} was obtained for the $^5A_1$-$^5A_2$ transition. The calculation predicts a positive sign for the ΔE_Q, in agreement with the sign experimentally determined by Wiedenmann et al. (1986).

For Fe^{2+} at M1, an effective axial crystal field was assumed. By adopting the experimentally known positive sign of V_{ZZ} in the ΔE_Q for M1, a pseudotetragonal distortion can be predicted. The ground-state splitting Δ was used as an adjustable parameter, yielding $\Delta = 480$ cm^{-1}. The fitted covalency factor was $\alpha^2 = 0.72$ for M1 as well as M2.

The isomer shifts of Fe^{2+}(M1) and Fe^{2+}(M2) at 0 K were determined using the Debye approximation. The estimated Debye temperatures, θ_D, for M1 and M2 are 325 ± 25 K and 225 ± 25 K, respectively.

INTRODUCTION

The local electronic states of Fe^{2+} ions in orthopyroxene, $(Fe,Mg)SiO_3$, and related properties have been the subject of several studies. The space group of orthopyroxene is *Pbca*. Generally, Fe and Mg are distributed over two nonequivalent, octahedrally coordinated positions of equal multiplicity, M1 and M2, with Fe exhibiting some preference for M2. The point symmetry of M1 and M2 is 1.

Runciman et al. (1973) explained the spin-allowed spectrum by assuming a pseudosymmetry of *mm*2 (C_{2v}) for the crystal field seen by the Fe^{2+} ion at the M2 site. With reference to their observation of a band in the infrared region near 2350 cm^{-1}, Goldman and Rossman (1977) reexamined this problem using the same model, but included the fourth-order terms of the crystal field potential, which had been neglected by Runciman et al. (1973). They assigned the three observed bands at 11000, 5400, and 2350 cm^{-1} to the transitions $^5A_1$-$^5A_1$, $^5A_1$-$^5B_1$, and $^5A_1$-$^5B_2$, respectively.

A frequency of 354 cm^{-1} for the transition from the electronic ground state $^5A_1$ to the first excited state, $^5A_2$, was predicted. Although this assignment is now generally accepted, there is some disagreement about that of the bands caused by Fe^{2+} at M1 (cf. Burns, 1970; Goldman and Rossman, 1979; Steffen et al., 1988; and references therein). Recently, Steffen et al. (1988) studied the electronic spectra of a series of synthetic orthopyroxene samples to clarify the situation. By assuming an approximate symmetry of $4/mmm$ (D_{4h}) for the M1 octahedron, they assigned the bands at 11000 and 8500 cm^{-1} to the $^5B_{2g}$-$^5A_{1g}$ and $^5B_{2g}$-$^5B_{1g}$ transitions, respectively.

At present, however, our knowledge about the electronic states of Fe^{2+} in orthopyroxene is still incomplete because the energy intervals between the electronic ground states and first excited states of both Fe^{2+}(M1) and Fe^{2+}(M2) have never been determined experimentally. Since such information is important for the understanding of the magnetic properties and ^{57}Fe hyperfine interactions in orthopyroxene, which have been investigated in some detail by Wiedenmann et al. (1986) and Stanek and Hafner (1988), it is desirable to define more precisely the crystal field experienced by Fe^{2+} at M1 and M2, as well as the electronic states.

We have therefore measured the Mössbauer effect of ^{57}Fe in two synthetic samples of orthopyroxene between 7 and 293 K to obtain the temperature dependence of the hyperfine data. These have been interpreted in terms of crystal field theory by assuming a pseudosymmetry of *mm*2 for M2 and an effective axial symmetry for M1.

* Present address: Guangzou Branch, Institute of Geochemistry, Academia Sinica, Guangzhou 510640, China.
** Present address: Max-Planck-Institut für Chemie, Postfach 3060, 6500 Mainz, Germany.

0003–004X/93/0102–0008$02.00

TABLE 1. Chemical composition, lattice parameters, and unit-cell volume of orthopyroxenes Opx6, Fe/(Fe + Mg) = 0.80, and Opx4, Fe/(Fe + Mg) = 0.51

Sample	x^*	a (Å)	b (Å)	c (Å)	V (Å^3)
Opx6	0.80	18.372(5)	9.009(3)	5.229(3)	865.41
Opx4	0.51	18.328(3)	8.945(2)	5.218(2)	855.36

Note: Standard deviations of the lattice parameters are given in parentheses.

* x = Fe/(Fe + Mg).

EXPERIMENTAL

Two Fe-rich orthopyroxene samples, Opx6 ($Fe_{0.80}Mg_{0.20}SiO_3$) and Opx4 ($Fe_{0.51}Mg_{0.49}SiO_3$) were synthesized at 900 °C and 3 GPa by use of a 3000-ton multianvil press. Cu tubes were loaded with spectroscopically pure MgO, SiO_2, Fe_2O_3, and metallic Fe powder in appropriate proportions (Peng et al., 1986). Scanning electron microscope photographs revealed very small amounts of quartz present after synthesis (less than 1% by volume). The cell dimensions were determined from 16 unambiguously identified X-ray reflections by the least-squares method. Chemical compositions determined by wet chemical analyses and lattice parameters are presented in Table 1.

The ^{57}Fe resonant absorption spectra were recorded by a conventional method: an electromechanical Doppler velocity system operated at constant acceleration using a symmetrical velocity wave form, in conjunction with a 1024 channel analyzer. Approximately 0.5×10^6 counts per channel were accumulated for each spectrum. A ^{57}Co source of nominally 40 mCi in Rh, kept at 293 K for all experiments, was used. The Doppler velocity scale was calibrated with spectra of a metallic Fe foil (thickness 0.03 mm). The orthopyroxene absorbers were prepared by mixing the sample with sugar and pressing the mixture into Cu rings with an inner diameter of 7 mm (absorber area 0.4 cm^2). Their concentration was approximately 5 mg natural Fe per cm^2. For temperature control, a gas-flow cryostat operated with liquified He at temperatures below 78 K and liquified N_2 at temperatures between 78 and 293 K was used. The absorber temperatures were measured with C or Pt resistors mounted at the Cu ring. The temperature was determined with a precision of ±1 K between 7 and 120 K, and ±3 K between 120 and 293 K.

The symmetrical spectra were folded to 512 channels with a program based on the least-squares technique for determination of the point of zero velocity. The folded spectra were fitted assuming four Lorentzian peaks without constraints.

RESULTS

The ^{57}Fe quadrupole splitting, ΔE_Q

The ^{57}Fe resonant absorption spectra of orthopyroxene between 7 and 293 K of this study correspond, in principle, to those described first by Virgo and Hafner (1968) and Shenoy et al. (1969). A typical spectrum is shown in Figure 1. The quadrupole splittings, ΔE_Q, of the M1 and M2 doublets exhibit different temperature dependencies. Whereas ΔE_Q(M1) significantly increases with decreasing temperature below 293 K, ΔE_Q(M2) remains more or less independent of temperature. This distinct behavior yields an apparently different resolution of the two partly overlapping doublets at different temperatures.

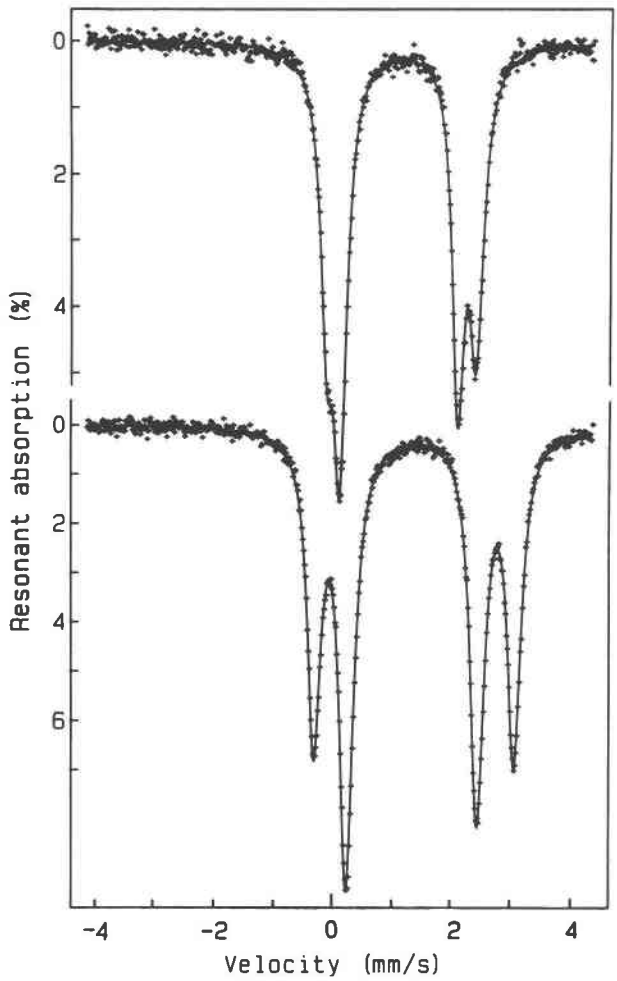

Fig. 1. The ^{57}Fe spectrum of the paramagnetic phase of synthetic orthopyroxene $Fe^{2+}/(Fe^{2+} + Mg^{2+}) = 0.80$ (Opx6). Upper spectrum: absorber at 293 K; lower spectrum: absorber at 44.5 K. The two outer lines are due to Fe^{2+} at position M1; the two inner lines are due to Fe^{2+} at position M2.

Sample Opx6 ($Fe_{0.80}Mg_{0.20}SiO_3$) exhibited a sharp Néel point, T_N, at 28 K (onset of magnetic hyperfine splitting), in agreement with Shenoy et al. (1969). It was possible to fit the two partly overlapping doublets between 28 and 293 K with good precision. Below 28 K, fitting is complex because of the magnetic splitting into 16 lines. It was difficult to obtain precise fits because of the rapidly changing magnetization over a small range of temperatures (strong overlap of most of the magnetic lines between 7 and 28 K). The ΔE_Q values (including the signs

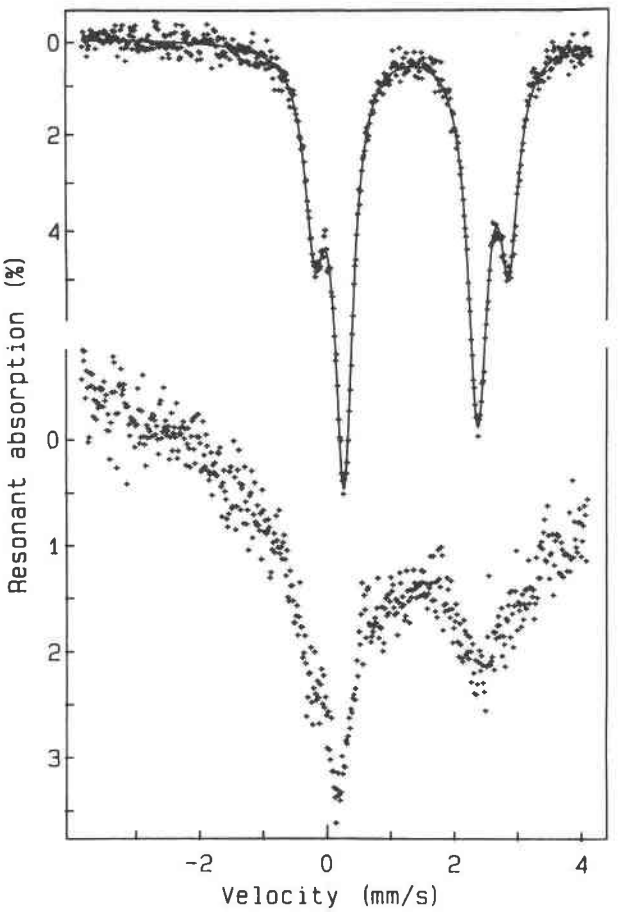

Fig. 2. The ^{57}Fe spectrum of synthetic orthopyroxene $Fe^{2+}/(Fe^{2+} + Mg^{2+}) = 0.51$ (Opx4). Upper spectrum: absorber at 12.5 K (paramagnetic phase); lower spectrum: absorber at 7.5 K (superparamagnetic phase).

of the electric field gradients) and center shifts of the magnetic phase of $FeSiO_3$ orthopyroxene at 4.2 K were determined by Wiedenmann et al. (1986). The somewhat increased line widths of Opx6 at 28 K are interpreted in terms of some heterogeneous chemical or temperature distribution over the absorber at an average temperature immediately above T_N. The line widths of the four-line fit of the spectrum at 293 K were also found to be slightly increased, probably because of the shoulder effect (cf. Opx4, next paragraph below).

Sample Opx4 ($Fe_{0.51}Mg_{0.49}SiO_3$) showed a gradual increase of the line widths for both doublets when cooled between 20 and 7 K because of paramagnetic relaxation effects (Fig. 2), but no Néel point was observed. This behavior is in agreement with Shenoy et al. (1969). The ΔE_Q and the center position, δ, of the doublets could therefore be studied with precision only between 12.5 K and 175 K. Above 175 K, the overlap of the two doublets is significant, with the result that simple Lorentzian fits do not provide line positions with sufficient precision. Because of its low intensity in orthopyroxenes with higher Mg contents, the M1 doublet occurs as a rather weak shoulder of the intense M2 doublet. The non-Lorentzian character of the M2 curve shape may, therefore, produce a large systematic error in the fitted value of $\Delta E_Q(M1)$. Fitting the spectrum with the transmission integral would probably yield more adequate data, but this was not attempted.

Both samples (Opx6 and Opx4) exhibited a very small resonant absorption line near +0.8 mm/s because of paramagnetic Fe^{3+} ions, probably located at the M1 position. This was not accounted for in our four-line fits.

The M1 and M2 doublets generally displayed somewhat asymmetric intensities for the high- and low-energy peaks, as is typically observed in spectra of polycrystalline pyroxene absorbers. For chemical compositions similar to that of Opx6, the asymmetry effect could be studied over a larger temperature range with precision. Our count rates were not high enough to allow a quantitative analysis of the effect, although the asymmetry was found to be quite independent of temperature, indicating some texture in the absorber. For our determination of the line positions, the effect was negligible.

The ^{57}Fe isomer shift

The center shift, $\delta(T,P)$, of the ^{57}Fe spectrum (in our case M1 or M2 doublet) is often designated as "isomer shift". Here T is the temperature and P the pressure. In the following we want to consider mainly the dependence of δ on the temperature at ambient pressure in more detail; $\delta(T)$ at constant pressure may be written:

$$\delta(T) = \delta_0 + \delta_C(T) + \delta_{SOD}(T). \quad (1)$$

In Equation 1, $\delta_0 = \alpha\rho(0)$ is the intrinsic isomer shift at 0 K, with $\rho(0)$ being the electron density at the atomic radius $r = 0$ and α a nuclear constant with a negative sign for ^{57}Fe. The temperature-dependent part of the intrinsic isomer shift is $\delta_C(T)$, and the second-order Doppler shift is δ_{SOD}. There are two contributions that mainly make up δ_C:

$$\delta_C(T) = \delta_i(T) + \delta_e(T). \quad (2)$$

The value $\delta_i(T)$ is the contribution to $\rho(0)$ due to changes in the polyhedral volume and ligand bonding because of thermal lattice expansion. The contribution due to thermal population of the spin-orbit states is δ_e, which may change 4s and 3d populations.

Within the Debye approximation, δ_{SOD} may be formulated as

$$\delta_{SOD} = -\frac{3kT}{2Mc}\left[\frac{3\Theta_D}{8T} + f(T/\theta_D)\right] \quad (3)$$

where

$$f(T/\theta_D) = 3(T/\theta_D)_3 \int_0^{\theta_D/T} x^3(e^x - 1)^{-1}\,dx \quad (4)$$

is the Debye function. Inserting the values for the Boltzmann constant, k, the velocity of light, c, and the ^{57}Fe

TABLE 2. Hyperfine parameters of orthopyroxenes Opx6, Fe/(Fe + Mg) = 0.80, and Opx6, Fe = 0.51

T	δ*		ΔE_Q**		Line widths†			
(K)	M1 (mm/s)	M2 (mm/s)	M1 (mm/s)	M2 (mm/s)	(mm/s)	(mm/s)	(mm/s)	(mm/s)
				Opx6				
28	1.306	1.276	3.131	2.047	0.298	0.278	0.289	0.254
45	1.307	1.275	3.135	2.043	0.253	0.272	0.270	0.254
79	1.299	1.264	3.123	2.035	0.253	0.274	0.268	0.258
120	1.283	1.245	3.083	2.028	0.254	0.278	0.271	0.254
175	1.253	1.211	2.948	2.016	0.258	0.281	0.276	0.258
215	1.226	1.184	2.810	2.003	0.265	0.284	0.280	0.277
293	1.180	1.139	2.496	1.971	0.285	0.258	0.250	0.279
				Opx4				
12	1.296	1.278	3.048	2.099	0.373	0.354	0.372	0.339
20	1.299	1.278	3.060	2.094	0.343	0.324	0.331	0.305
45	1.296	1.277	3.075	2.086	0.290	0.302	0.302	0.288
77	1.295	1.270	3.068	2.077	0.284	0.275	0.274	0.278
100	1.290	1.263	3.053	2.074	0.282	0.272	0.273	0.273
203	1.237	1.202	2.798	2.053	0.305	0.305	0.278	0.253

* Referred to a metallic Fe absorber at 293 K; standard deviations ±0.001 mm/s, total error ±0.005 mm/s.
** Standard deviations ±0.002 mm/s, total error ±0.005 mm/s.
† Standard deviations ±0.005 mm/s, total error ±0.020 mm/s.

nuclear mass, M, into Equation 3, the relation for δ_{SOD} may be written (Wegener, 1966; Shenoy et al., 1978):

$$\delta_{SOD}(T) = -2.74 \cdot 10^{-4}\theta_D - 7.30 \cdot 10^{-4} T f(T/\theta_D). \quad (5)$$

In Equation 5, δ_{SOD} is in mm/s, and T in K. In the temperature range of our data, δ_{SOD} provides the primary contribution to the total thermal shift of δ. It has a quasi-linear dependency on the temperature, especially at temperatures higher than about 120 K (cf. Fig. 3). At temperatures much lower than θ_D, the dependency is predicted to be significantly reduced, according to Equation 5. With the assumption that θ_D at M1 and M2 in orthopyroxene is higher than 120 K, $\delta_C(T)$ must also have a linear dependence on the temperature above 120 K, as inspection of Figure 3 shows. It may be written approximately

$$\delta_C(T) = CT. \quad (6)$$

The function $\delta(T)$ was fitted to the data of Table 2 by solving Equations 1, 5, and 6 and using δ_0, C, and θ_D as fitting parameters. This was carried out by iteration on the basis of the least-squares principle. For the Debye function (Eq. 4) values of Beattie (1926) were used. The most probable values for δ_0, C, and θ_D obtained for M1 and M2 in sample Opx6 are presented in Table 3, and the final functions, $\delta(T)$, plotted in Figure 3. For sample Opx4, the data were not sufficient to compute fits.

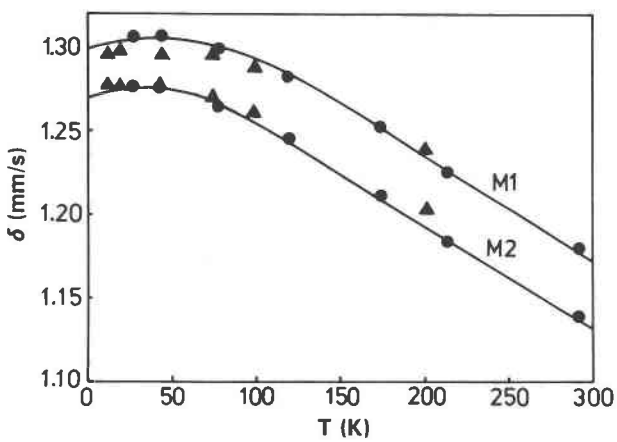

Fig. 3. Dependence of the isomer shift (δ) of orthopyroxene on temperature, T. Circles: $Fe^{2+}/(Fe^{2+} + Mg^{2+}) = 0.80$ (Opx6), $T_N = 28$ K. Below T_N, accurate determination of δ from the 16-line magnetic spectrum was not possible. Triangles: $Fe^{2+}/(Fe^{2+} + Mg^{2+}) = 0.51$ (Opx4), no sharp T_N; below 12.5 K superparamagnetic (cf., Fig. 1). The solid lines were fitted by use of Eqs. 1, 5, 6, and the data of Table 3.

CRYSTAL FIELD ANALYSIS

Hyperfine data for pyroxenes may be obtained theoretically using ab initio computations of the electron and spin-density distributions of atomic clusters. Here, however, we want to use crystal field theory mainly to focus on the external point charge and valence electron contribution to the electric field gradient (EFG). In the present work the term "electric field gradient" is used for the positive second derivative, V_{ij} ($i, j = x, y, z$) of the electrostatic potential V. Spin-orbit coupling will be included in our calculation. Runciman et al. (1973) computed crystal field energies by means of the weak field scheme, taking into account second-order terms only. They did

TABLE 3. Fitted values of δ_0, C, and θ_D for Fe^{2+} in orthopyroxene Opx6, Fe/(Fe + Mg) = 0.80

Atom site	δ_0* (mm/s)	C (10^{-5} mm/s K)	θ_D (K)
M1	1.395	+3.7 ± 2.0	325 ± 25
M2	1.337	+7.0 ± 1.8	225 ± 25

* Refers to a metallic Fe absorber at 293 K. The estimated total error is ±0.005 mm/s.

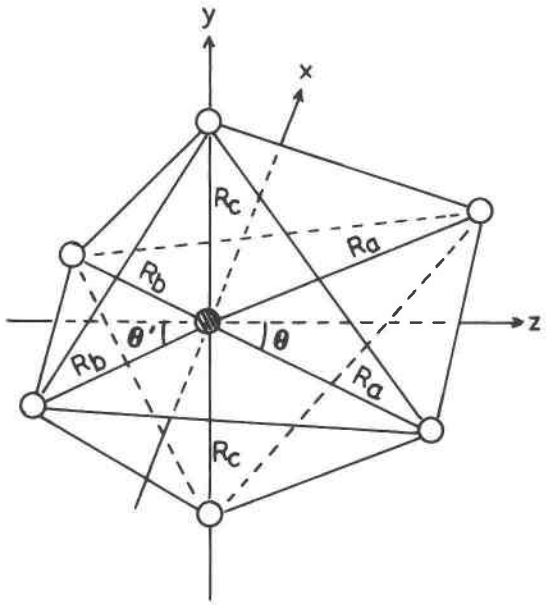

Fig. 4. Geometry of the distorted coordination octahedron M2: R_a = ½(2.161 + 2.130) = 2.146 Å, R_b = ½(2.444 + 2.576) = 2.510 Å, R_c = ½(1.997 + 2.035) = 2.016 Å, θ = 35.8°, θ' = 41.4°. The parameters were used to compute the terms A_{kl} of Eq. 7; interatomic distances from Burnham et al. (1971).

account for the spin-orbit contribution, but their assignment of the band at 3100 cm^{-1} was incorrect. Goldman and Rossman (1977) employed the operator-equivalent method, including fourth-order terms, but they did not consider spin-orbit coupling.

The geometry of the M2 octahedron is shown in Figure 4, which illustrates the significant distortion. Runciman et al. (1973) noticed that the major distortion of M2 is due to the elongation of the M2-O3A and M2-O3B bonds and the reduced O3A-M2-O3B angle (atomic designations after Burnham et al., 1971). Hence the appropriate pseudosymmetry of the M2 octahedron is *mm*2, the quasi-twofold axis being the bisector of the O3A-M2-O3B angle. That direction was taken to be the **z** axis of the crystal field at the M2 site. The **y** axis was assumed to be in the plane formed by M2-O2B and **z.**

For Fe^{2+} at the M1 position, an effective crystal field of axial symmetry was assumed. Both tetragonally and trigonally distorted crystal fields yield the same relationship between ΔE_Q and temperature, but the signs of the EFG (signs of the maximum eigenvalue V_{ZZ} of V_{ij}) differ.

Fe^{2+} at the M2 sites

Crystal field perturbation. The crystal-field potential energy at the M2 sites may be written as

$$Vc = \sqrt{4\pi}\, ze^2 \sum_i \{r_i^2[A_{20}Z_{20}(\theta_i,\phi_i) + A_{22}^c Z_{22}^c(\theta_i,\phi_i)] + r_i^4[A_{40}Z_{40}(\theta_i,\phi_i) + A_{42}^c Z_{42}^c(\theta_i,\phi_i) + A_{44}^c Z_{44}^c(\theta_i,\phi_i)]\} \quad (7)$$

where ze is the effective charge of the ligands, $Z_{kl}(\theta_i,\phi_i)$ the tesseral harmonics, and r_i, θ_i, ϕ_i the coordinates of the ith electron. The expressions for the coefficients A_{kl} in Equation 7 as functions of the ligand coordinates can be derived using the method described by Griffith (1961). With the adoption of the equivalent hole formulation, the wave functions $\phi_i(M_S)$ (M_S = −2, −1, 0, 1, 2), classified according to the irreducible representations of the point group *mm*2, are the following linear combinations of Slater determinants:

$$\begin{aligned} B_2: &\quad \phi_\xi(2) = |\eta\zeta\theta\epsilon| \\ B_1: &\quad \phi_\eta(2) = |\zeta\theta\epsilon\xi| \\ A_2: &\quad \phi_\zeta(2) = |\theta\epsilon\xi\eta| \\ A_1: &\quad \phi_\theta(2) = |\epsilon\xi\eta\zeta| \\ &\quad \phi_\epsilon(2) = |\xi\eta\zeta\theta| \end{aligned} \quad (8)$$

where ξ, η, ζ, θ, and ϵ represent one-electron wave functions d_{yz}, d_{zx}, d_{xy}, d_{z^2}, and $d_{x^2-y^2}$, respectively. One may easily obtain $\phi_k(M_S)$ with $M < 2$ by applying the descending operator, $L_- = L_x - iL_y$, on $\phi_k(2)$. The wave functions correct to the first order obtained by diagonalizing the crystal field perturbation matrix are

$$\begin{aligned} &\phi_+ = (\cos x)\,\phi_\theta + (\sin x)\,\phi_\epsilon, \\ &\phi_- = (\sin x)\,\phi_\theta - (\cos x)\,\phi_\epsilon,\ \phi_\xi,\ \phi_\eta, \text{ and } \phi_\zeta \end{aligned} \quad (9)$$

where x is defined by

$$\tan(2x) = 2\langle\phi_\theta|V_c|\phi_\epsilon\rangle/(\langle\phi_\theta|V_c|\phi_\theta\rangle - \langle\phi_\epsilon|V_c|\phi_\epsilon\rangle). \quad (10)$$

Spin-orbit coupling. We are now in a position to consider the spin-orbit coupling. The corresponding Hamiltonian is

$$\mathcal{H} = \sum_i \xi(\gamma_i)\,\hat{I}_i\cdot\hat{S}_i. \quad (11)$$

Where $\hat{I}_i$ and $\hat{S}_i$ are the orbital momentum and spin operators of the ith electron. Since the states ϕ_η and ϕ_- lie much higher in energy than the ground state, ϕ_+, they can be safely neglected. The spin-orbit coupling matrix is Hermitian, with the basis $\phi_k(M_S)$ (k = +, ζ, ξ; M_S = 0, ±1, ±2). In order to transform it into a real matrix, a unitary transformation may be performed according to

$$[\chi_1(M_s),\ \chi_2(M_s),\ \chi_3(M_s)] = [\phi_+(M_s),\ \phi_\zeta(M_s),\ \phi_\xi(M_s)]\begin{bmatrix} 1 & & \\ & i & \\ & & -i \end{bmatrix}. \quad (12)$$

The spin-orbit coupling matrix with the new basis is given in Appendix 1.[1]

[1] Copies of Appendix Tables 1 and 2 may be ordered as Document AM-93-516 from the Business Office, Mineralogical Society of America, 1130 Seventeenth Street NW, Suite 330, Washington, DC 20036, U.S.A. Please remit $5.00 in advance for the microfiche.

TABLE 4. Crystal field transition frequencies (cm^{-1}) of Fe^{2+}(M2)

Transition		Obs I*	Obs II**	Calc†
$^5A_1$	$^5A_2$	—	—	817
$^5A_1$	$^5B_2$	2350	—	2715
$^5A_1$	$^5B_1$	5400	4910	4936
$^5A_1$	$^5A_1$	10930	10700	10679

* Measured for $Fe_{0.14}Mg_{0.86}SiO_3$ (Goldman and Rossman, 1977).
** Measured for $Fe_{0.86}Mg_{0.14}SiO_3$ (Burns, 1970).
† With $Ze^2\langle r^2\rangle = -2.7$ a.u. and $Ze^2\langle r^4\rangle = -21.0$ a.u. (this work).

Electric field gradient, electronic part. Because of the spin-orbit interaction, the possible states of the system are linear combinations of $\chi_i(M_S)$:

$$\psi_i = \sum_{k=1}^{15} c_{ki} \, |k\rangle \tag{13}$$

Here we designate $\chi_i(M_s)$ as $|k\rangle$ for brevity. The expectation value of the EFG operator, $V^{val}_{\alpha\beta}$, in the state ψ_i is given by

$$\langle V^{val}_{\alpha\beta}\rangle_i \equiv \langle\psi_i|V^{val}_{\alpha\beta}|\psi_i\rangle = \sum_k \sum_l c_{ki}c_{li}\langle k|V^{val}_{\alpha\beta}|l\rangle \tag{14}$$

where $\langle k|V^{val}_{\alpha\beta}|l\rangle$ are the matrix elements of $V^{val}_{\alpha\beta}$ with the basis $\chi_i(M_s)(i = 1, 2, 3; M_s = 0, 1, 2)$. They are listed in Appendix 2. Thus, the valence electron contribution to the EFG is given by

$$\langle V^{val}_{\alpha\beta}\rangle_{av} = \sum_i \langle V^{val}_{\alpha\beta}\rangle_i \exp(-E_i/kT) \Big/ \sum_i \exp(-E_i/kT) \tag{15}$$

where E_i is the energy of the state ψ_i.

Lattice field gradient. The lattice contribution to the EFG may be obtained by differentiating the crystal field potential $V = -V_C/e$, i.e.,

$$V^{lat}_{xx} = \sqrt{5}ze(A_{20} - \sqrt{3}A^c_{22})$$
$$= \sqrt{5}a_2(A_{20} - \sqrt{3}A^c_{22})/e\langle r^2\rangle \tag{16}$$
$$V^{lat}_{yy} = \sqrt{5}ze(A_{20} + \sqrt{3}A^c_{22})$$
$$= \sqrt{5}a_2(A_{20} + \sqrt{3}A^c_{22})/e\langle r^2\rangle \tag{17}$$
$$V^{lat}_{zz} = -\sqrt{5}zeA_{20} = -\sqrt{5}a_2A_{20}/e\langle r^2\rangle \tag{18}$$
$$V^{lat}_{\alpha\beta} = 0 \qquad (\alpha \neq \beta) \tag{19}$$

where $a_2 = ze^2\langle r^2\rangle$.

Nuclear quadrupole splitting, ΔE_Q. The principal values of the EFG tensor may be obtained by diagonalizing the matrix $(1 - R)\langle V^{val}_{\alpha\beta}\rangle_{av} + (1 - \gamma_\infty)V^{lat}_{\alpha\beta}$, where R and γ_∞ are the Sternheimer shielding and antishielding factors, respectively. If we label the principal axes (X, Y, Z) of the EFG tensor in such a way that $V_{ZZ} \geq V_{XX} \geq V_{YY}$, the nuclear quadrupole interaction energy is formulated as

$$\Delta E_Q = \tfrac{1}{2}eV_{ZZ}Q(1 + \eta^2/3)^{1/2} \tag{20}$$

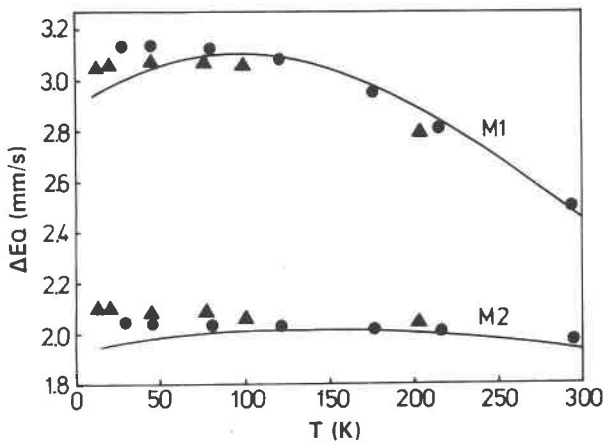

Fig. 5. Dependence of the ^{57}Fe quadrupole splitting (ΔE_Q) of Fe^{2+} at M1 and M2 on temperature, T, in orthopyroxene. Circles: $Fe^{2+}/(Fe^{2+} + Mg^{2+}) = 0.80$ (Opx6). Triangles: $Fe^{2+}/(Fe^{2+} + Mg^{2+}) = 0.51$ (Opx4). The solid lines are calculated by use of crystal field analysis.

where Q is the nuclear quadrupole moment and $\eta = (V_{XX} - V_{YY})/V_{ZZ}$ the asymmetry parameter. The values of Q, $\langle r^{3-}\rangle$, $\langle r^2\rangle$, R, and γ_∞ used here are those of the free Fe^{2+} ion and the same as those used by Ingalls (1964), i.e., $Q = 0.29$ barn, $\langle r^{3-}\rangle = 4.8$ a.u., $\langle r^2\rangle = 1.4$ a.u., $R = 0.32$, and $\gamma_\infty = -11$. The covalency factor, α^2, may be introduced to relate the spin-orbit coupling constant, λ, of Fe^{2+} in the crystal to that of free Fe^{2+}, λ_0: $\lambda = \alpha^2\lambda_0$. Using α^2, $a_2 = ze^2\langle r^2\rangle$, and $a_4 = ze^2\langle r^4\rangle$ as adjustable parameters, the ΔE_Q values of Fe^{2+}(M2) were calculated. For this calculation, bond distances and bond angles were taken from Burnham et al. (1971). The best agreement with experimental data was obtained with $\alpha^2 = 0.725$, $a_2 = -2.7$ a.u. and $a_4 = -21.0$ a.u. The calculated crystal-field transition frequencies, together with those reported in the literature, are listed in Table 4. The calculated ΔE_Q values for Fe^{2+}(M2) are shown in Figure 5.

Fe^{2+} at the M1 sites

For the ΔE_Q of Fe^{2+}(M1), the method of calculation is essentially the same as that described for Fe^{2+}(M2), except that instead of a_2 and a_4, the ground-state splitting of Fe^{2+}(M1), Δ, was used as the fitting parameter. The calculated ΔE_Q values for Fe^{2+}(M1) with $\alpha^2 = 0.72$ and $\Delta = 480$ cm^{-1}, are also shown in Figure 5.

DISCUSSION

Our crystal field calculations confirmed that the $mm2$ pseudosymmetry assumption for Fe^{2+} ions at the M2 sites used for explaining the optical absorption spectra (Runciman et al., 1973; Goldman and Rossman, 1979) is also a good model for the interpretation of the ^{57}Fe resonant absorption data of orthopyroxene (cf. Figs. 3, 5). The calculated dependence of ΔE_Q on temperature between 4.2 and 300 K is in reasonably good agreement with that observed. Moreover, the calculations predict a positive sign for V_{ZZ} at M2, in accordance with that determined

experimentally from the magnetic ^{57}Fe spectrum of polycrystalline orthoferrosilite at 4.2 K (Wiedenmann et al., 1986) and a single-crystal study of the paramagnetic ^{57}Fe spectrum of orthoenstatite at 300 K (Stanek and Hafner, 1988). The calculated value for the asymmetry parameter at 300 K ($\eta = 0.16$) is somewhat smaller than the experimental values of $\eta = 0.35$ in orthoferrosilite at 4.2 K (Wiedenmann et al., 1986) and $\eta = 0.20 \pm 0.07$ in orthoenstatite at 300 K (Stanek and Hafner, 1988). It should be noted, however, that the ^{57}Fe spectrum is generally not very sensitive to η, and so the experimental determination of η from ^{57}Fe data is not very precise.

Our calculations show, however, that the frequency, Δ_1, of the transition from the ground state of Fe^{2+}(M2) to its first excited state is about 800 cm^{-1} (Table 4), i.e., much larger than that predicted previously (354 cm^{-1}) by Goldman and Rossman (1977).

The experimentally observed ΔE_Q dependence of Fe^{2+}(M1) on the temperature can be reasonably well accounted for, if an axially symmetric crystal field is assumed. Adoption of a trigonal as well as a tetragonal distortion yields similar relationships of ΔE_Q vs. temperature, but the predicted sign for the ΔE_Q is opposite. Since a tetragonal crystal field yields a positive sign, in agreement with Wiedenmann et al. (1986), the crystal field at M1 seen by Fe^{2+} must be of a quasi-tetragonal symmetry. The site occupancy of Fe^{2+} at M1 in the orthoenstatite studied by Stanek and Hafner (1988) was not high enough to allow an unambiguous determination of the sign at that position.

The splitting of the ground state of Fe^{2+} derived from the temperature dependence of ΔE_Q is about 480 cm^{-1}, i.e., more than three times greater than the value of 150 cm^{-1} proposed by Steffen et al. (1988).

Our determined values of δ_0 for the Fe^{2+} isomer shift at M1 and M2 are consistent with the local geometrical configuration of the respective polyhedra. The δ_0 data in Table 3 may be compared, for example, with $\delta_0 = 1.612$ (± 0.09) mm/s (referred to metallic Fe) of $^{[6]}Fe^{2+}$ in FeF_2 (Reschke et al., 1977). Although the covalent participation in the Fe-O bonding of chain silicates is significantly greater than that in the Fe-F bonding of fluorides, the Fe^{2+} bonds in pyroxene are still primarily ionic.

Many data on ^{57}Fe isomer shifts of silicates determined at ambient temperature have been reported in the literature. A review of those values in terms of chemical bonding is not possible, since precise information on the thermal shifts between 4.2 and 300 K is needed in order to determine the characteristic Debye temperatures, θ_D, and C parameters of the thermal contribution to the isomer shift. Our present data on orthopyroxene confirm, however, previous conclusions from studies at 78 K that δ_0 of Fe^{2+} at M2 is somewhat smaller than δ_0 of Fe^{2+} at M1, in accordance with the more distorted geometry and the smaller M-O2B and M-O2A distances of the M2 octahedron compared with M-O1B and M-O1A distances of M1.

Although more thermal data on δ of Fe^{2+} in chain silicates with different chemical compositions, especially on θ_D and C are highly desirable, it may be speculated that the temperature dependence of δ, e.g., for octahedrally coordinated Fe^{2+} in chain silicates, may be rather similar. Our values of $\theta_D = 325$ K for M1 and $\theta_D = 225$ K for M2 (sample Opx6) are somewhat lower than the value 561 K $> \theta_D >$ 484 K obtained for FeF_2 by Reschke et al. (1977). In spite of the rather large error of the fitted θ_D (cf. Table 3), the small difference in the relationship of δ vs. temperature at M1 and M2 appears to be established, yielding a somewhat higher θ_D for M1. The curvatures in the temperature region below 20 K in Figure 3 should be interpreted with caution for two reasons: (1) the transition to the magnetically ordered phase of sample Opx6, and (2) approximations adopted in Equation 5. The total error for the δ_0 values in Table 3 is estimated to be ± 0.005 mm/s.

Acknowledgments

We thank Hongsen Xie, Institute of Geochemistry, Academia Sinica, Guiyang, for high-pressure synthesis of orthopyroxene, the late Klaus Fecher, Marburg, for SEM measurements, and Gertrud Steinbach and F.A. Amiri, Marburg, for technical assistance. C.L. thanks Academia Sinica for granting a fellowship for six months at the University of Marburg.

This paper was presented at the 15th General Meeting of the International Mineralogical Association, Physics of Minerals Symposium, Beijing, China, June 28–July 3, 1990.

References cited

Beattie, J.R. (1926) Six place tables of the Debye energy and specific heat functions. Journal of Mathematics and Physics, 6, 1–32.

Burnham, C.W., Ohashi, Y., Hafner, S.S., and Virgo, D. (1971) Cation distribution and atomic vibrations in an iron-rich orthopyroxene. American Mineralogist, 56, 850–876.

Burns, R.G. (1970) Mineralogical applications of crystal field theory, p. 87–92. Cambridge University Press, London.

Goldman, D.S., and Rossman, G.R. (1977) The spectra of iron in orthopyroxene revisited: The splitting of the ground state. American Mineralogist, 62, 151–157.

——— (1979) Determination of quantitative cation distribution in orthopyroxenes from electronic absorption spectra. Physics and Chemistry of Minerals, 4, 43–53.

Griffith, J.S. (1961) The theory of transition metal ions, p. 199–205. Cambridge University Press, London.

Ingalls, R. (1964) Electric field gradient tensor in ferrous compounds. Physical Review, 133A, 787–795.

Peng, W., Xie, H., Zhang, Y., and Xu, H. (1986) A study of the orthopyroxene series synthesized under high pressure. Acta Mineralogica Sinica, 6, 308–314 (in Chinese).

Reschke, R., Trautwein, A., and Harris, F.E. (1977) Electronic structure, pressure- and temperature-dependent charge densities, and electric field gradients in FeF_2. Physical Review, 15B, 2708–2717.

Runciman, W.A., Sengupta, D., and Marshall, M. (1973) The polarized spectra of iron in silicate. I. Enstatite. American Mineralogist, 58, 444–450.

Shenoy, G.K., Kalvius, G.M., and Hafner, S.S. (1969) Magnetic behavior of the $FeSiO_3$-$MgSiO_3$ orthopyroxene system from NGR in ^{57}Fe. Journal of Applied Physics, 40, 1314–1316.

Shenoy, G.K., Wagner, F.E., and Kalvius, G.M. (1978) The measurement of isomer shifts. In G.K. Shenoy, and F.E. Wagner, Eds., Mössbauer isomer shifts, p. 101–107. North-Holland Publishing Company, Amsterdam.

Stanek, J., and Hafner, S.S. (1988) Electric field gradient tensors of ^{57}Fe in orthorhombic $(Mg,Fe)SiO_3$. Hyperfine Interactions, 39, 235–252.

Steffen, G., Langer, K., and Seifert, F. (1988) Polarized electronic absorp-

tion spectra of synthetic (Mg,Fe)-orthopyroxenes, ferrosilite and Fe^{3+}-bearing ferrosilite. Physics and Chemistry of Minerals, 16, 120–129.

Virgo, D., and Hafner, S.S. (1968) Re-evaluation of the cation distribution in orthopyroxenes by the Mössbauer effect. Earth and Plantary Science Letters, 4, 265–269.

Wegener, H. (1966) Der Mössbauer-Effekt. Bibliographisches Institut—Taschenbuch 2/2a, Mannheim, Germany.

Wiedenmann, A., Regnard, J.-R., Fillion, G., and Hafner, S.S. (1986) Magnetic properties and magnetic ordering of the orthopyroxenes $Fe_xMg_{1-x}SiO_3$. Journal of Physics C: Solid State Physics, 19, 3683–3695.

Manuscript received June 10, 1991
Manuscript accepted August 20, 1992